Scilight

International Journal of Transportation and Logistics Research
https://www.sciltp.com/journals/ijtlr



Article

Check for updates

Joint Vessel Sequencing and Discrete Speed Optimization under Speed-Dependent Safety Headways

Chongwei Gong [1], Yue Liu [2] and Yusheng Zhou [1,*]

[1] Department of Logistics and Maritime Studies, The Hong Kong Polytechnic University, Hong Kong SAR, China
[2] Faculty of Information, Liaoning University, Shenyang 110036, China
* Correspondence: yusheng1.zhou@polyu.edu.hk

How To Cite: Gong, C.; Liu, Y.; Zhou, Y. Joint Vessel Sequencing and Discrete Speed Optimization under Speed-Dependent Safety Headways. *International Journal of Transportation and Logistics Research* **2026**, *2*(2), 4. https://doi.org/10.53941/ijtlr.2026.100010

Received: 12 August 2026
Revised: 18 November 2026
Accepted: 18 November 2026
Published: 25 November 2026

Abstract: Single-lane bidirectional port channels serve one traffic direction at a time, making vessel scheduling essential for reducing waiting. However, sailing speed affects both transit time and the separation required between successive vessels. We therefore formulate a continuous-time mixed-integer linear programming (MILP) model to optimise vessel sequencing and discrete speed selection. The model assigns channel entry times to minimise the sum of total waiting time and a weighted speed penalty. Specifically, safety headways depend on the selected speeds of both the leading and following vessels, maintaining the prescribed separation throughout transit. In addition, opposing vessels enter after the channel has cleared and the direction change buffer has elapsed. To solve this model, we develop a sequence and speed alternating improvement (SSAI) algorithm that adjusts vessel order and speed under the same safety constraints. Tests against operational baselines showed lower mean waiting, while 40 comparisons against exact solutions yielded a mean objective gap of 3.92%. These results support coordinated vessel release and speed planning, with safety intervals determined by the selected speeds.

Keywords: port channel; vessel scheduling; vessel sequencing; discrete speed selection; mixed integer linear programming

1. Introduction

Maritime transport underpins international trade by moving goods between markets worldwide. Ports connect these flows to inland transport, making efficient vessel access essential to their gateway role [1]. In a single-lane bidirectional port channel, arriving vessels share the passage with departing vessels. Only one direction can use the channel at a time, while following vessels must maintain safe separation. However, each release delays opposing vessels, while speed changes affect when following vessels can enter. These dependencies make vessel release difficult to coordinate in port traffic management.

In practice, these release decisions must also account for access rules that vary with vessel size [2,3]. For example, Zhanjiang's approved channel design requires tidal passage in one direction for fully laden 300,000-tonne vessels, while allowing smaller bulk carriers to pass bidirectionally [3]. Moreover, release planning becomes important when many vessels share a restricted waterway. The Kiel Canal, where large opposing vessels can meet only in designated sidings, recorded 22,262 ship passages in 2025 [2,4,5]. In addition, reconstructions of its 2007 traffic indicate daily mean waiting times on the order of tens of minutes [2]. More recently, Shenzhen's Tonggu Channel has illustrated the value of reducing waiting through improved scheduling. A 2026 official report describes reductions of 32.9% and 44.2% in total waiting before channel entry across two three-month operational datasets [6]. These examples therefore highlight the value of coordinating release plans with vessel speeds and access conditions while maintaining safe separation.

Vessel scheduling in ports with single-lane bidirectional channels has been widely studied. For example, Lalla-Ruiz et al. [7] formulated the waterway ship scheduling problem to coordinate incoming and outgoing

Copyright: © 2026 by the authors. This is an open access article under the terms and conditions of the Creative Commons Attribution (CC BY) license (https://creativecommons.org/licenses/by/4.0/).
Publisher's Note: Scilight stays neutral with regard to jurisdictional claims in published maps and institutional affiliations.

vessels while minimising waiting. Their mathematical model and heuristics allocate passage opportunities across restricted waterways, establishing channel access as a shared resource. Hill et al. [8] reformulated this problem as a multimode project scheduling model in which vessel movements compete for resources with changing availability. This compact integer programming formulation improved exact solution efficiency and solved the existing literature instances to optimality. These studies show how an explicit representation of channel occupancy supports systematic release decisions. Canal models further specify where vessels can wait to allow opposing traffic to pass [2,4]. Beyond channel access, Liu et al. [9] integrated berth allocation with vessel sequencing while accounting for heterogeneous sailing speeds. The resulting plans link channel use to berth service, showing why the release sequence must be evaluated alongside terminal operations. Related studies examined how wider port activities [10–16] and tidal access windows [17–21] further restrict feasible release times. In addition, Gan et al. [22] improved online sequencing by shifting vessel positions according to differences in sailing time. Their sliding window handles traffic uncertainty while limiting the computational effort required to update the schedule. Fuzzy scheduling further represented uncertain passage times [23], while reinforcement learning improved the choice of release sequence [24]. Collectively, these studies establish that passage times affect vessel order and the allocation of available entry opportunities. However, shorter passage alone does not imply that successive vessels can safely enter at shorter intervals, because their separation also depends on relative motion. Safe release therefore requires entry headways that remain consistent with the sailing speeds selected for successive vessels.

Matching headways to the selected speeds requires speed optimisation to consider how successive vessels interact throughout their passage. Earlier research by Fagerholt et al. [25] established the value of speed optimisation for reducing fuel consumption while respecting service time windows. In port operations, Xia et al. [26] combined scheduling with speed reduction to improve traffic efficiency while reducing emissions. More recent studies integrated speed decisions with berth allocation and vessel sequencing [27], or with scheduling in compound channels [28]. This body of work supports evaluating speed within the operating schedule rather than treating faster transit as an isolated improvement. However, changing speed also alters the relative motion of successive vessels and therefore the interval needed to maintain safe separation. For example, a faster follower can progressively close on a slower leader despite having sufficient separation when entering the channel. A headway calibrated at normal speed may consequently be insufficient for this combination, while imposing unnecessary waiting on another. Moreover, Liu et al. [29] showed that checks at channel boundaries can miss unsafe separation during transit when vessel speeds vary. Their use of whole voyage constraints highlights why safety must be related to vessel motion throughout the shared passage. For discrete speed instructions, this means evaluating the headway for the selected speeds of both the leader and follower. Reducing one vessel's passage time cannot be assessed independently of the resulting entry opportunities for the vessels that follow. Otherwise, excessive spacing wastes channel capacity, whereas an underestimated interval can make an apparently efficient release plan unsafe. Joint optimisation therefore requires a sequencing model in which each discrete speed choice is matched to a physically consistent safety headway.

To address the coupling between vessel order and speed-dependent safety headways, we propose a framework that jointly optimises vessel sequencing and discrete speed selection. First, we formulate a continuous-time mixed-integer linear programming (MILP) model that determines the vessel sequence and assigns channel entry times and speed levels. Its objective balances total waiting time against a normalised speed penalty. Specifically, pairwise safety headways are derived from relative vessel motion, linking the selected speeds to channel occupancy and safe entry spacing. Precomputation and exact linearisation incorporate these relationships while preserving the model's linear structure. Next, we develop the sequence and speed alternating improvement (SSAI) algorithm using the same objective and safety rules as the MILP. The search alternates between adjusting individual speeds and revising vessel order, rebuilding each candidate at its earliest feasible entry times. A dynamic safety audit then verifies the resulting schedule against the headways associated with its vessel order and selected speeds. In addition, progressive baseline comparisons separate the benefits of speed selection from those of direction grouping and further sequence improvement. Exact validation and sensitivity tests further assess solution quality and performance under different operating conditions. Finally, the experiments show that SSAI achieves lower observed mean waiting than the operational baselines and a low average optimality gap in exact validation.

Section 2 presents the problem setting, formulates the joint optimisation model and explains the SSAI algorithm. Section 3 describes the experimental design and evaluates performance through baseline comparisons, exact validation and sensitivity analysis. Section 4 interprets the findings and discusses their practical implications for channel scheduling. Finally, Section 5 summarises the main conclusions and outlines managerial recommendations and future research directions.

2. Methodology

The method links each vessel release decision to the channel occupancy and separation requirements that it must satisfy. First, we define the operating setting and notation, then derive transit times and safety headways for each discrete speed combination. These quantities enter a continuous-time MILP through precomputation and exact linearisation, with a finite Big M derived from the planning horizon. Finally, SSAI searches for schedules under the same formulation, and a dynamic safety audit checks each resulting release plan.

2.1. Problem Definition and Notation

2.1.1. Operating Setting and Modelling Scope

This study considers a port channel with one lane shared by inbound and outbound vessels. The channel serves one traffic direction at a time, so opposing vessels cannot occupy it simultaneously. However, vessels moving in the same direction may enter consecutively if they satisfy the prescribed longitudinal safety headway. Release also depends on vessel readiness, which determines the earliest permissible channel entry time. For an inbound vessel, this is its arrival time at the waiting area outside the channel entrance. By contrast, an outbound vessel becomes ready once cargo handling has finished and all departure preparations, including unberthing, are complete. Each vessel selects an economic, normal or fast speed before entry and maintains that speed throughout transit. Accordingly, the model determines when and in which order vessels enter, while selecting speeds to balance waiting against the normalised speed penalty.

Within this setting, the model adopts a deterministic static formulation over a fixed planning horizon. The information required to schedule each vessel is known before planning begins, and all vessels must complete transit within that horizon. Vessels may be resequenced in designated holding areas before release, after which their passage follows the assigned order. Ready times connect berth operations to channel scheduling by specifying when vessels become available for release. In addition, the available speed levels and prescribed safety buffers define the operating conditions used to construct feasible schedules.

2.1.2. Sets, Indices, and Parameters

Channel scheduling must distinguish following movements from opposing traffic because the two interactions require different safety rules. Let $\mathcal{N}$ denote the set of vessels to be scheduled, indexed by i and j, with $\mathcal{N}^{\text{in}}$ and $\mathcal{N}^{\text{out}}$ representing inbound and outbound vessels, respectively. For each vessel i, $\mathcal{K}_i$ contains the available discrete speed levels. The ordering relationships between vessels are represented by the following set of unordered pairs:

$$\mathcal{P} = \{(i,j) \mid i,j \in \mathcal{N}, i < j\}. \tag{1}$$

To apply the appropriate safety rule, $\mathcal{P}$ is partitioned according to whether the two vessels travel in the same or opposite directions:

$$\mathcal{P}^S = \{(i,j) \in \mathcal{P} \mid d_i = d_j\}, \tag{2}$$

$$\mathcal{P}^O = \{(i,j) \in \mathcal{P} \mid d_i \neq d_j\}. \tag{3}$$

The condition $i < j$ assigns one ordering decision to each pair, while the partition determines the safety rule attached to that decision. Pairs in $\mathcal{P}^S$ require a following headway, whereas pairs in $\mathcal{P}^O$ require the channel to clear before opposing traffic enters. These disjoint subsets jointly cover $\mathcal{P}$, so every vessel pair is linked to its corresponding safety requirement. Table 1 summarises the parameters used to express these requirements. Unless stated otherwise, time is measured in minutes (min), speed in knots (kn), and distance in nautical miles (nmi).

A release decision must also account for how long each vessel occupies the channel. For a channel of length L, the transit time of vessel i at speed level k therefore follows from the selected speed v_{ik}:

$$p_{ik} = \frac{60L}{v_{ik}}, \forall i \in \mathcal{N}, k \in \mathcal{K}_i. \tag{4}$$

The factor 60 in Equations (4) to (7) converts hours to minutes, because distances are in nautical miles and speeds are in nautical miles per hour (knots). Thus, each available speed level has a known transit time that enters the scheduling model as a constant. Faster transit can release channel capacity sooner, but its benefit must be assessed alongside the speed penalty. Moreover, the selected speeds determine how closely vessels can safely enter, motivating the headway derivation in the next subsection.

Table 1. Main parameters and definitions.

Parameter	Definition
a_i	Ready time of vessel i (min)
d_i	Sailing direction of vessel i
L	Channel length (nmi)
v_{ik}	Speed of vessel i at level k (kn)
p_{ik}	Channel transit time of vessel i at level k (min)
D_{ij}	Minimum longitudinal safety distance when vessel i leads vessel j (nmi)
g_i	Type of vessel i
l_i	Length of vessel i, measured in metres (m)
$\beta_{g_i g_j}$	Safety distance multiplier for the ordered type pair (g_i, g_j)
h_{ij}^{kl}	Minimum safe entry headway for leader i at level k and follower j at level l (min)
ε_{ij}	Additional safety time buffer for vessel pair (i, j) (min)
c_{ik}	Normalised speed penalty of vessel i at level k (dimensionless)
δ	Direction change buffer (min)
H	Upper bound of the planning horizon (min)
M	Big M constant used to relax inactive sequencing constraints (min)
α	Weight converting a unit speed penalty to equivalent waiting time (min)
R	Maximum number of complete SSAI improvement iterations
ρ	Maximum vessel displacement in the insertion neighbourhood (positions)

2.2. Construction of Safety Headways That Depend on Speed

Closely spaced vessel releases can reduce waiting, but they must preserve the required separation while vessels share the channel. However, a gap that is sufficient at entry may shrink when the follower travels faster than its leader. We therefore determine the required entry interval by considering separation both when the follower enters and when the leader exits.

To derive this interval, consider two vessels travelling in the same direction. Vessel i travels at speed level k and leads vessel j, which travels at level l. Their entry times are T_i and T_j, so the leader travels for $T_j - T_i$ minutes before the follower enters. At the follower's entry, the leader must have covered at least the prescribed distance D_{ij}. Using the leader's speed v_{ik}, this requirement gives the following lower bound on the entry interval:

$$T_j - T_i \geq \frac{60 D_{ij}}{v_{ik}}. \tag{5}$$

However, satisfying Equation (5) at entry does not prevent a faster follower from reducing the separation during transit. When $v_{jl} > v_{ik}$, the minimum separation during overlapping channel occupancy occurs immediately before the leader exits. At the leader's exit time $T_i + p_{ik}$, the follower must therefore have travelled no farther than $L - D_{ij}$. Rearranging this condition gives a second lower bound on the entry interval:

$$T_j - T_i \geq p_{ik} - \frac{60(L - D_{ij})}{v_{jl}}. \tag{6}$$

The two bounds jointly specify the entry interval needed to maintain the prescribed separation at both ends of overlapping transit. We then add the operational buffer ε_{ij} to obtain the safety headway for vessel i leading vessel j:

$$h_{ij}^{kl} = max\left\{\frac{60 D_{ij}}{v_{ik}}, p_{ik} - \frac{60(L - D_{ij})}{v_{jl}}\right\} + \varepsilon_{ij}. \tag{7}$$

In Equation (7), the first term controls separation at follower entry, whereas the second controls separation immediately before leader exit. Because both vessels maintain constant speeds, their separation changes linearly during overlapping occupancy. Consequently, satisfying the two endpoint conditions also maintains the prescribed distance throughout that overlap. The buffer ε_{ij} provides an additional time allowance for operational error and simplified vessel motion. It is measured in minutes and added once, after taking the maximum of the two bounds. In general, $h_{ij}^{kl} \neq h_{ji}^{lk}$, so reversing the vessel order can change the required entry interval. Thus, the scheduling benefit of a speed choice depends on which vessel leads and which follows.

To specify the distance requirement, D_{ij} is scaled by vessel size and the ordered combination of vessel types. The lengths l_i and l_j determine the base distance, while the dimensionless coefficient $\beta_{g_i g_j}$ adjusts it. The distance satisfies $0 \leq D_{ij} < L$, so the prescribed separation fits within the channel. The distance is calculated as follows:

$$D_{ij} = \frac{\beta_{g_i g_j} max\{l_i, l_j\}}{1852}. \tag{8}$$

Equation (8) uses the greater vessel length, so pairs involving a larger vessel receive a larger base distance. The type multiplier further adjusts this distance for the ordered vessel pair. Because vessel lengths are measured in metres, division by 1852 converts the distance to nautical miles using 1 nmi = 1852 m. For each vessel order and available speed combination, the inputs to Equation (7) are known before scheduling. Thus, all safety headways can be precomputed and used as constant coefficients in the MILP. These coefficients allow the joint model to evaluate shorter channel occupancy alongside the entry intervals required for safe following.

2.3. Joint Vessel Sequencing and Discrete Speed Model

The headways derived above specify safe intervals between following vessels, but reducing total waiting requires coordination across the complete schedule. A speed choice can shorten one vessel's channel occupancy while changing the time at which another vessel may enter. Consequently, its scheduling benefit depends on the release order and the speeds assigned to other vessels. We therefore formulate a MILP in continuous time to determine when each vessel enters and which speed it uses. These entry decisions are linked by sequencing constraints, which apply the relevant headway to following vessels and require clearance before opposing traffic enters. Figure 1 shows how this model connects to SSAI and the dynamic safety audit to produce and check a vessel release schedule.

2.3.1. Decision Variables

Each vessel's release time must be consistent with the speed it uses and the vessels that pass before it. To represent the timing of vessel i, the model first introduces the following nonnegative continuous variables:

$$T_i \geq 0, C_i \geq 0, W_i \geq 0, \tag{9}$$

where T_i denotes channel entry time, while C_i records when vessel i leaves the channel. The variable W_i measures the delay between readiness and entry, linking the release decision to the objective. Because transit duration depends on speed, the timing variables are linked to a discrete speed choice. Accordingly, the binary variable z_{ik} identifies whether vessel i uses speed level k, as defined below:

$$z_{ik} = \begin{cases} 1, & \text{vessel } i \text{ selects speed level } k, \\ 0, & \text{otherwise.} \end{cases} \tag{10}$$

Next, the model records which vessel receives channel access first within each pair. For $(i,j) \in \mathcal{P}$, this relative order is represented by the binary variable y_{ij}:

$$y_{ij} = \begin{cases} 1, & \text{vessel } i \text{ passes before vessel } j, \\ 0, & \text{vessel } j \text{ passes before vessel } i. \end{cases} \tag{11}$$

The following headway also depends on the speed levels selected by the two vessels. For each pair $(i,j) \in \mathcal{P}^S$, the auxiliary binary variable q_{ij}^{kl} identifies the selected combination of levels $k \in \mathcal{K}_i$ and $l \in \mathcal{K}_j$:

$$q_{ij}^{kl} = \begin{cases} 1, & \text{vessels } i \text{ and } j \text{ select levels } k \text{ and } l, \\ 0, & \text{otherwise.} \end{cases} \tag{12}$$

The variable q_{ij}^{kl} represents the product $z_{ik}z_{jl}$, so it identifies the speed combination selected for the two vessels. The constraints below express this relationship linearly and apply the appropriate headway according to the selected passage order. This representation links release timing to the vessel movements that determine safe channel access.

2.3.2. Objective Function

Choosing higher speeds can shorten channel occupancy, but the associated operating burden must also enter the scheduling decision. We therefore minimise a weighted sum of total waiting and the normalised speed penalty, using Z to denote the objective value:

$$minZ = \sum_{i\in\mathcal{N}} W_i + \alpha \sum_{i\in\mathcal{N}} \sum_{k\in\mathcal{K}_i} c_{ik}\, z_{ik}. \tag{13}$$

The first term in Equation (13) measures the total time that vessels wait between becoming ready and entering the channel. In the second term, z_{ik} activates the dimensionless penalty c_{ik} for the speed level assigned to vessel i. Parameter α converts this penalty to a waiting time equivalent, allowing both terms to be compared on the same scale. A larger α places more weight on avoiding speed penalties, whereas a smaller value gives greater priority to reducing waiting. Section 3.1.2 specifies how c_{ik} is calculated from the available speed levels. Consequently,

the model evaluates whether the reduction in total waiting justifies the additional weighted penalty associated with a speed increase.

2.3.3. Constraint System

Reducing waiting requires a release plan that coordinates vessel movements within the channel's operating rules. The constraints first establish when each vessel can move and how long it occupies the channel at the selected speed. They then apply following headways or require full channel clearance, depending on the directions of the two vessels. Finally, the planning horizon bounds the complete schedule, while the variable domains distinguish discrete choices from continuous timing decisions.

(1) Basic Time Relationships and Speed Selection

In the schedule, readiness sets the earliest entry time, while the selected speed determines how long each vessel occupies the channel. Accordingly, each vessel must enter no earlier than its ready time and select exactly one permitted speed level. The selected duration then fixes exit time, whereas the difference between entry and readiness gives waiting time. The following constraints express these linked requirements for every scheduled vessel:

$$T_i \geq a_i, \forall i \in \mathcal{N}. \tag{14}$$

$$\sum_{k \in \mathcal{K}_i} z_{ik} = 1, \forall i \in \mathcal{N}. \tag{15}$$

$$C_i = T_i + \sum_{k \in \mathcal{K}_i} p_{ik}\, z_{ik}, \forall i \in \mathcal{N}. \tag{16}$$

$$W_i = T_i - a_i, \forall i \in \mathcal{N}. \tag{17}$$

Equations (14) to (17) thus connect each selected speed to a complete channel movement and its waiting contribution. The readiness condition also makes waiting nonnegative, so the objective measures delay after the vessel becomes available. The following constraints use these individual timings to coordinate shared channel access.

(2) Linearisation of Speed Combinations

The headway between following vessels must match the speeds selected for both vessels in a pair. To select the corresponding precomputed coefficient, q_{ij}^{kl} must equal the product $z_{ik}z_{jl}$. For every $(i,j) \in \mathcal{P}^S$, $k \in \mathcal{K}_i$ and $l \in \mathcal{K}_j$, the model imposes this relationship through three linear constraints:

$$q_{ij}^{kl} \leq z_{ik}, \tag{18}$$

$$q_{ij}^{kl} \leq z_{jl}, \tag{19}$$

$$q_{ij}^{kl} \geq z_{ik} + z_{jl} - 1. \tag{20}$$

Equations (18) and (19) set the auxiliary variable to zero when either corresponding speed level is not selected. Conversely, Equation (20) sets it to one when both speed levels are selected. In conjunction with Equation (15), these conditions identify exactly one realised speed combination for each pair in $\mathcal{P}^S$. The safety constraint can therefore use a linear weighted sum to apply the headway associated with that combination.

(3) Same Direction Safety Headways

The selected speed combination determines the headway needed to maintain separation between following vessels. For each $(i,j) \in \mathcal{P}^S$, vessel i can lead vessel j only if the following entry condition is satisfied:

$$T_j \geq T_i + \sum_{k \in \mathcal{K}_i} \sum_{l \in \mathcal{K}_j} h_{ij}^{kl}\, q_{ij}^{kl} - M(1 - y_{ij}). \tag{21}$$

Conversely, when vessel j leads vessel i, the model applies the headway for the reversed order:

$$T_i \geq T_j + \sum_{k \in \mathcal{K}_i} \sum_{l \in \mathcal{K}_j} h_{ji}^{lk}\, q_{ij}^{kl} - M y_{ij}. \tag{22}$$

When $y_{ij} = 1$, Equation (21) requires vessel j to enter at least the selected headway after vessel i. Equation (22) is relaxed in this case by its Big M term. When $y_{ij} = 0$, the active condition instead becomes Equation (22), with vessel j leading vessel i. Thus, the model applies the interval associated with the realised leader and follower, including their selected speeds. Because reversing the order can change the headway, these alternatives allow sequencing and speed choices to influence the same release decision. These complementary constraints maintain the required longitudinal separation while allowing compatible vessels to share the channel.

(4) Opposite Direction Conflict Resolution

Opposing vessels require a different access rule because they cannot occupy the channel simultaneously. Instead of a following headway, the next movement must wait for channel clearance and the direction change buffer. For $(i,j) \in \mathcal{P}^O$, vessel i may pass first under the following clearance condition:

$$T_j \geq C_i + \delta - M(1 - y_{ij}). \tag{23}$$

Conversely, when vessel j passes first, the model requires the corresponding clearance before vessel i enters:

$$T_i \geq C_j + \delta - My_{ij}. \tag{24}$$

When $y_{ij} = 1$, Equation (23) makes vessel j wait until vessel i has exited and the buffer δ has elapsed. Equation (24) is relaxed, so it does not impose the opposite passage order. When $y_{ij} = 0$, these roles are reversed and Equation (24) governs the release of vessel i. The two constraints jointly separate opposing movements and reserve the prescribed time for changing the traffic direction. Consequently, the timing of direction changes follows from the vessel schedule, allowing compatible movements to be grouped through optimisation.

(5) Planning Horizon and Variable Domains

Finally, all scheduled movements must finish within the planning horizon used to define the optimisation problem. The following bounds keep each vessel's entry and exit times within that horizon:

$$0 \leq T_i \leq H, 0 \leq C_i \leq H, \forall i \in \mathcal{N}. \tag{25}$$

In addition, the variable domains distinguish the discrete operational choices from the continuous timing decisions:

$$z_{ik} \in \{0,1\}, \forall i \in \mathcal{N}, k \in \mathcal{K}_i, \tag{26}$$

$$y_{ij} \in \{0,1\}, \forall (i,j) \in \mathcal{P}, \tag{27}$$

$$q_{ij}^{kl} \in \{0,1\}, \forall (i,j) \in \mathcal{P}^S, k \in \mathcal{K}_i, l \in \mathcal{K}_j. \tag{28}$$

$$T_i, C_i, W_i \geq 0, \forall i \in \mathcal{N}. \tag{29}$$

Equation (25) bounds channel occupancy over the planning horizon, while Equations (26) to (28) identify the binary decisions. Equation (29) requires nonnegative times and is consistent with the readiness and waiting relationships. These finite bounds also support the construction of Big M, as explained in Section 2.4. As a system, the constraints connect each selected speed to a feasible release time and coordinate the resulting vessel movements within the shared channel.

2.4. Linearisation Properties and Big M Specification

Each pair of sequencing constraints must enforce the selected passage order while leaving the alternative order inactive. A finite planning horizon provides the time bounds needed to choose a valid Big M. We first construct this horizon from the vessel data and the precomputed safety headways. Let $p^{max} = max_{i,k} p_{ik}$ denote the longest available transit time, and define $s^{max} = max\{h^{max}, p^{max} + \delta\}$. The latter covers both following headways and the time required for channel clearance before a direction change. Starting at the latest ready time, consecutive entries separated by s^{max} therefore accommodate every vessel in a serial schedule. Adding the final vessel's transit time gives the following horizon bound:

$$H = max_{i \in \mathcal{N}} a_i + (n-1)s^{max} + p^{max},$$

where $n = |\mathcal{N}|$ is the number of vessels, and h^{max} is the maximum headway defined in Equation (31). For any available speed assignment, this serial construction completes all vessel movements within H. If $\mathcal{P}^S$ is empty, h^{max} is set to zero.

With $0 \leq T_i, C_i \leq H$, the largest difference between the relevant timing variables is bounded by H. Consequently, relaxing a following constraint requires $M \geq H + h^{max}$, whereas relaxing an opposing clearance constraint requires $M \geq H + \delta$. A common value that satisfies both requirements is therefore chosen as follows:

$$M = H + max\{h^{max}, \delta\}, \tag{30}$$

where the maximum headway includes both possible vessel orders and all available speed combinations:

$$h^{max} = max_{(i,j) \in \mathcal{P}^S, k \in \mathcal{K}_i, l \in \mathcal{K}_j} max\{h_{ij}^{kl}, h_{ji}^{lk}\}. \tag{31}$$

The headways in Equation (31) already include the operational buffer from Equation (7). Therefore, h^{max} enters the horizon bound through s^{max} and determines the required relaxation margin for following vessels in Equation (30). For opposing vessels, C_i already accounts for transit duration, so the additional margin is the direction

change buffer δ. Moreover, p_{ik}, h_{ij}^{kl} and c_{ik} are precomputed constants for the finite sets of available speeds. Combined with Equations (18) to (20), these constants keep the complete formulation linear in its decision variables. The resulting MILP provides a consistent formulation of safe vessel release for the solution procedure described next.

2.5. Sequence and Speed Alternating Improvement Algorithm

An effective release plan must coordinate vessel order with the speeds that determine channel occupancy and safety headways. SSAI addresses this coupling by alternating adjustments to speed and sequence, using the same objective and safety constraints as the MILP. The resulting search balances the waiting associated with the release order against the weighted penalty for the selected speeds.

To represent these decisions, let $S = (\pi, \ell)$ denote a candidate schedule, where $\pi = (\pi_1, \dots, \pi_n)$ gives the vessel order. For vessel i, the component $\ell_i \in \mathcal{K}_i$ specifies its speed level, and $t_i(S)$ denotes its entry time. The exit time $C_i(S)$ then follows from that entry time and the selected transit duration:

$$S = (\pi, \ell), C_i(S) = t_i(S) + p_{i\ell_i}, \ell_i \in \mathcal{K}_i. \tag{32}$$

Once order and speeds are fixed, channel access requirements determine the earliest feasible entry for each vessel. First, the vessel must be ready, and all preceding opposing vessels must have cleared the channel with the required buffer. In addition, its entry must respect the safety headways associated with preceding vessels moving in the same direction. For the vessel at position $r = 1, \dots, n$, these requirements give the following recursion:

$$t_{\pi_r}(S) = max\left\{a_{\pi_r}, \max_{\substack{q<r \\ d_{\pi_q} \neq d_{\pi_r}}} \left[C_{\pi_q}(S) + \delta\right], \max_{\substack{q<r \\ d_{\pi_q} = d_{\pi_r}}} \left[t_{\pi_q}(S) + h_{\pi_q \pi_r}^{\ell_{\pi_q} \ell_{\pi_r}}\right]\right\}, \tag{33}$$

where the maximum over an empty set is defined as minus infinity. Because the recursion includes every preceding vessel, a local change can propagate through later entry times. The reconstructed schedule is evaluated using the same waiting and speed penalties as Equation (13):

$$Z(S) = \sum\nolimits_{i \in \mathcal{N}} \left[t_i(S) - a_i + \alpha c_{i\ell_i}\right]. \tag{34}$$

SSAI first tests changes to one vessel's speed level while holding the sequence fixed. This neighbourhood changes both transit duration and following headways, allowing the search to assess their combined effect on the objective:

$$\mathcal{N}_v(S) = \left\{(\pi, \ell'): \exists i \in \mathcal{N}, \ell_i' \in \mathcal{K}_i \setminus \{\ell_i\}, \ell_j' = \ell_j \; \forall j \neq i\right\}. \tag{35}$$

Next, bounded insertion moves a vessel from position r to a different position s, with both positions in $\{1, \dots, n\}$. The move is limited to ρ positions and evaluated after rebuilding the complete schedule. The experiments use $\rho = 5$, giving the following neighbourhood:

$$\mathcal{N}_I(S) = \{(ins_{r \to s}(\pi), \ell): r \neq s, |r - s| \leq \rho\}. \tag{36}$$

Finally, the direction block neighbourhood groups compatible movements to reduce repeated channel clearance. Let $\mathcal{B}(\pi)$ contain maximal blocks of consecutive vessels travelling in the same direction. For $B \in \mathcal{B}(\pi)$, $\mathcal{U}(B, \pi)$ contains positions immediately before and after the nearest other block in that direction. Distance is measured by block index, with ties choosing the earlier block. If none exists, $\mathcal{U}(B, \pi)$ is empty. Each move preserves the internal vessel order:

$$\mathcal{N}_B(S) = \{(reloc_{B \to u}(\pi), \ell): B \in \mathcal{B}(\pi), u \in \mathcal{U}(B, \pi)\}. \tag{37}$$

SSAI applies these neighbourhoods sequentially, using the updated candidate as the starting point for the next neighbourhood. At iteration m, the algorithm selects the best candidate from each neighbourhood, including the current schedule as a candidate, as expressed below:

$$S_m^v = \operatorname*{argmin}_{S' \in \mathcal{N}_v(S_m) \cup \{S_m\}} Z(S'). \tag{38a}$$

$$S_m^I = \operatorname*{argmin}_{S' \in \mathcal{N}_I(S_m^v) \cup \{S_m^v\}} Z(S'). \tag{38b}$$

$$S_m^B = \operatorname*{argmin}_{S' \in \mathcal{N}_B(S_m^I) \cup \{S_m^I\}} Z(S'). \tag{38c}$$

$$S_{m+1} = S_m^B \text{if } Z(S_m^B) < Z(S_m); S_{m+1} = S_m \text{otherwise.} \tag{38d}$$

Equation (38d) accepts an update only when it reduces the objective. Each neighbourhood retains the current schedule on a tie; other ties keep the first encountered candidate. The implementation accepts decreases greater than 10^{-8}. Consequently, the objective cannot increase, and the search stops when a complete iteration finds no improvement or the iteration limit R is reached.

Algorithm 1 first precomputes transit times and safety headways, then constructs two schedules in ready time order. S^{N} assigns normal speeds, whereas S^{G} chooses each vessel's level to minimise its own waiting plus weighted speed penalty, given preceding assignments. Each trial level uses Equation (33). SSAI selects the better schedule, choosing S^{G} on a tie, and applies the neighbourhood sequence. Enumeration follows vessel sequence order, the listed speed order and ascending target positions. This enumeration order and the tie rules above make the procedure deterministic for fixed inputs. The experiments use $R = 20$ and $\rho = 5$, as specified in Section 3.1.1.

Algorithm 1. Sequence and speed alternating improvement algorithm

Input Vessel data $\mathcal{N}, a_i, d_i, g_i, l_i, \mathcal{K}_i, v_{ik}, c_{ik}$; channel parameters $\beta_{g_i g_j}$, $L, \delta, \varepsilon_{ij}, \alpha$; iteration limit R; insertion radius ρ.

Output Validated $S^* = (\pi^*, \ell^*)$, with $T_i = t_i(S^*)$, $C_i = C_i(S^*)$, $W_i = T_i - a_i$, and $Z(S^*)$.

Precompute transit times and both ordered safety headways using Equations (4), (7) and (8).
Set $\pi^0 = sort_{(a_i,i)}(\mathcal{N})$.
Construct S^{N} and S^{G} under π^0 using the normal and greedy speed rules described above.
Set $S \leftarrow \mathrm{argmin}_{X \in \{S^{\mathrm{N}}, S^{\mathrm{G}}\}} Z(X)$.
for $m = 0, \ldots, R-1$ **do**
Set $S^{\mathrm{start}} \leftarrow S$.
for $v \in (v, I, B)$ **do** // speed, bounded insertion, direction block
Set $S^{\mathrm{best}} \leftarrow S$.
for each $X \in \mathcal{N}_v(S)$ **do**
Rebuild X and its entry and exit times using Equations (32) and (33).
Compute $Z(X)$ using Equation (34).
if $Z(X) < Z(S^{\mathrm{best}})$ **then**
Set $S^{\mathrm{best}} \leftarrow X$.
end if
end for
if $Z(S^{\mathrm{best}}) < Z(S)$ **then**
Set $S \leftarrow S^{\mathrm{best}}$.
end if
end for
if $Z(S) \geq Z(S^{\mathrm{start}})$ **then**
break
end if
end for
Set $S^* \leftarrow S$ and perform dynamic safety validation.
if any ready-time, same-direction, or opposite-direction constraint is violated **then**
Return infeasible status and the recorded validation errors.
else return S^*, T_i, C_i, waiting times, and $Z(S^*)$.
end if

Before the schedule is reported, the dynamic safety audit checks each movement against the model requirements. It first verifies that each entry respects vessel readiness and that opposing vessels never occupy the channel simultaneously. Next, it checks each realised headway using the selected passage order and the speeds assigned to the two vessels. The resulting output specifies when each vessel enters and leaves the channel, and which speed it follows. Waiting times and the objective are reported with the validation status.

Figure 1 integrates these components, from the operating inputs to the schedule checked by the dynamic safety audit. The resulting plan gives channel operators a coordinated release order, with entry times that reflect the selected speeds and required safety intervals. Thus, the method translates the joint decisions into a timetable that can be checked against the channel's operating rules. Section 3 evaluates whether this coordination reduces waiting under matched experimental conditions.

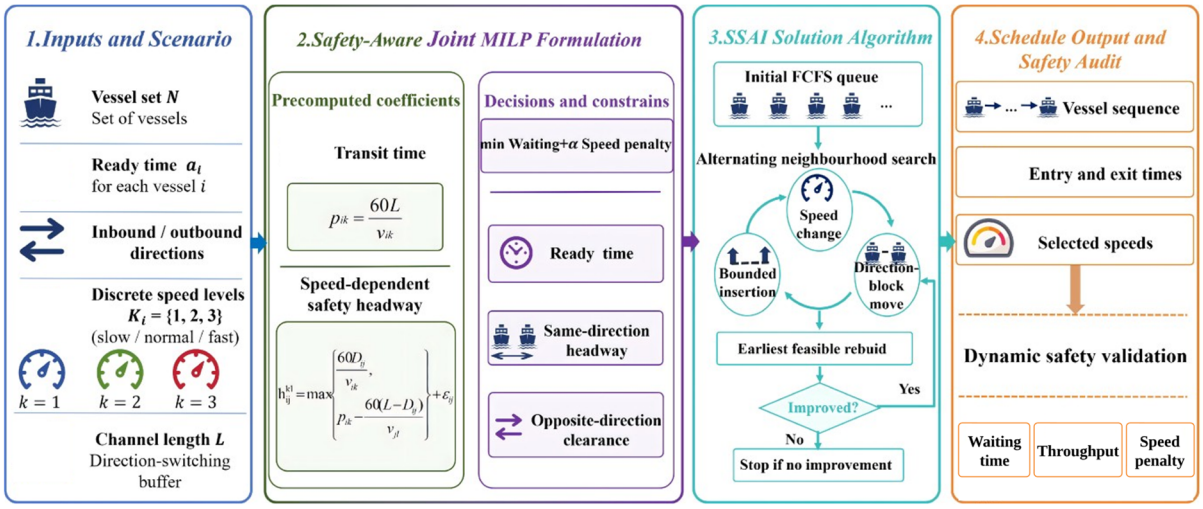

Figure 1. Four-stage architecture of the joint formulation and SSAI solution algorithm.

3. Experimental Design and Results

The experiments ask whether coordinating vessel order and speed improves channel use beyond speed adjustment or direction grouping alone. First, progressive baselines isolate these decisions, and small-scale exact solutions assess search quality. In addition, sensitivity tests examine safety distances and the objective weight. An engineering-parameter case then checks the same scheduling logic in a channel of practical scale. The evidence therefore links each computational comparison to a specific operational question.

3.1. Experimental Design and Configuration

To compare scheduling decisions under common operating conditions, all methods were evaluated on matched vessel instances. The following subsections describe the computing environment and instance generation before introducing the baselines and performance measures.

3.1.1. Computing Environment and Algorithm Settings

The experiments used a MacBook Air with an Apple M5 chip, a 10-core central processing unit and 16 GB of memory. The main implementation used Python 3.9.6, with NumPy 2.0.2 and Matplotlib 3.9.4 for data processing and plotting. SSAI used at most 20 improvement iterations and an insertion radius of five positions, stopping when a complete iteration found no improvement. Gurobi 12.0.3 computed reference optima only for exact validation, with a 120 s limit and a zero target mixed integer programming (MIP) gap. The additional objective weight sensitivity check used Python 3.12 with the same algorithm settings.

3.1.2. Instances and Parameter Settings

For a common traffic setting, the standard instances used a pooled Poisson ready time process with rate λ = 6 vessels/h across both directions. Table 2 lists the vessel lengths and available speed levels for each type. Independent exponential interarrival times had mean $60/\lambda$ = 10 min; their cumulative sums defined ready times rounded to 0.001 min. Direction and vessel type were sampled independently using the probabilities in Table 3.

Table 2. Vessel types and discrete speed settings.

Vessel Type	Length (m)	Economic Speed (kn)	Normal Speed (kn)	Fast Speed (kn)
Small	100	8	10	12
Medium	180	7	9	11
Large	280	6	8	10

The standard channel was 5 nmi long, with a 2 min direction change buffer and an additional 0.5 min buffer for following vessels. Both buffers were baseline scenario margins, with the direction change allowance applied after full channel clearance. For leader and follower types ordered as small, medium and large, the multiplier matrix had rows $(3.0, 3.5, 4.0)$, $(3.5, 4.0, 4.5)$ and $(4.0, 4.5, 5.0)$.

Fuel data for individual vessels were unavailable, so operating burden was represented by a cubic speed proxy. Normalising this proxy within each vessel's available levels gives a dimensionless penalty for comparing speed choices. The preference weight $\alpha = 0.15$ converts that penalty to equivalent waiting time. A unit increase in one vessel's penalty therefore contributes 0.15 min (9 s) to the objective. The normalised speed penalty is defined by the following expression:

$$c_{ik} = \frac{v_{ik}^3 - v_{i,min}^3}{v_{i,max}^3 - v_{i,min}^3},$$

where $v_{i,min}$ and $v_{i,max}$ denote the minimum and maximum available speeds of vessel i, respectively. Economic and fast speeds consequently receive penalties of 0 and 1, respectively. Table 3 summarises the baseline parameters, while Figure 2 illustrates the common channel operating setting.

Table 3. Baseline parameters for the standard instances.

Parameter	Baseline Value	Definition
Arrival rate λ	6 vessels/h	Total rate across both directions
Direction probabilities	0.5/0.5	Inbound/outbound
Vessel type probabilities	1/3/1/3/1/3	Small/medium/large
Speed penalty weight α	0.15 min	Waiting-time equivalent per penalty unit
Direction-change buffer δ	2 min	Additional margin after channel clearance
Same-direction buffer ε_{ij}	0.5 min	Added to every same-direction headway

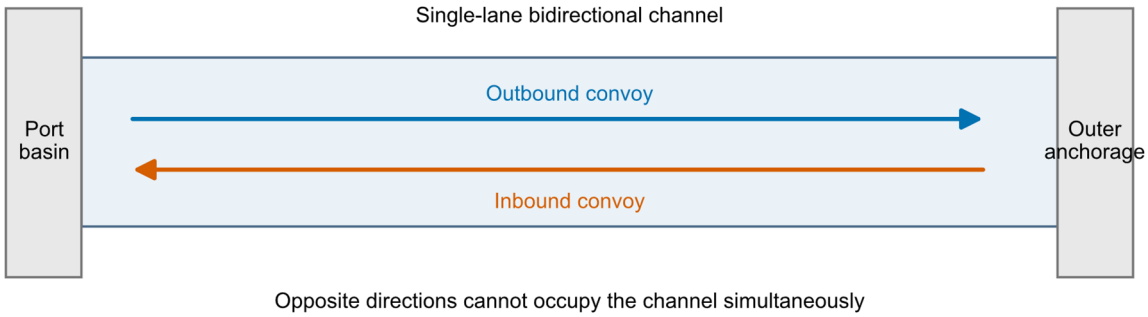

Figure 2. Operating scenario of a bidirectional channel with a single lane.

The standard comparisons used 10, 20, 30, 40 and 50 vessels, with ten instances per size generated from seeds 1 to 10. All methods were applied to the same 50 instances, so each comparison held vessel readiness and composition fixed. This matched design supports the progressively structured baseline comparison described next.

3.1.3. Algorithms and Baselines

The baselines progressively introduced speed choice and sequence flexibility to identify the contribution of each scheduling decision. First come, first served with fixed speed (FCFS-FS) followed ready time order at normal speed, using the corresponding reference headway. Next, first come, first served with discrete speed (FCFS-DS) retained the same order but improved individual speed choices using the realised headways.

Direction-grouped scheduling with discrete speed (DG-DS) then introduced sequencing through a deterministic lookahead of five vessels. It selected a vessel travelling in the current direction when available within that window, then improved speeds with the resulting order fixed. Both discrete speed baselines allowed at most 20 speed improvement iterations. In comparison, SSAI also used bounded insertions and direction block moves, rebuilding candidates with the headways defined in Section 2. The comparison therefore separates the benefits of speed selection from those of direction grouping and further sequence search.

3.1.4. Performance Measures

The evaluation measures assess whether each scheduling method reduces waiting while maintaining feasible channel access. Waiting performance was measured by total, mean and maximum waiting time, with schedule completion time and direction changes describing channel use. Throughput then measures the completed traffic over the scheduling interval and is expressed in vessels per hour as follows:

$$\text{Throughput} = \frac{|\mathcal{N}|}{max_{i\in\mathcal{N}} c_i - min_{i\in\mathcal{N}} a_i} \times 60, \tag{39}$$

where $|\mathcal{N}|$ is the number of vessels and the denominator is the elapsed time from the earliest ready time to the final channel exit. Because this interval is measured in minutes, multiplying by 60 expresses throughput in vessels per hour. Speed decisions were summarised by mean speed, the share assigned to each level and the normalised speed penalty. Computational effort was measured by wall clock time, and validation errors were recorded for each schedule. Each schedule was independently checked for readiness, realised safety headways and clearance between opposing vessels. These checks link the performance comparison to compliance with the channel's operating rules.

3.2. Primary Algorithm Performance

To assess the benefit of joint vessel sequencing and speed selection, we conducted a comparative experiment using the four scheduling methods. All methods used the 50 matched instances described in Section 3.1, covering 10 to 50 vessels with ten seeds at each size. The progressive baselines separated the effect of speed choice from the additional benefit of revising release order. Table 4 reports mean waiting, while Figure 3 relates waiting performance to runtime. Figures 4 and 5 then illustrate the resulting schedules and speed allocations.

Table 4. Waiting performance of the rule based scheduling methods.

Number of Vessels	FCFS-FS Mean Waiting (min)	FCFS-DS Mean Waiting (min)	DG-DS Mean Waiting (min)	SSAI Mean Waiting (min)	SSAI Reduction vs. DG-DS
10	36.52	25.56	18.48	11.67	36.9%
20	77.12	52.59	25.41	17.73	30.2%
30	129.08	90.14	31.01	21.16	31.8%
40	178.97	129.12	33.70	23.78	29.4%
50	228.71	169.82	36.26	25.12	30.7%

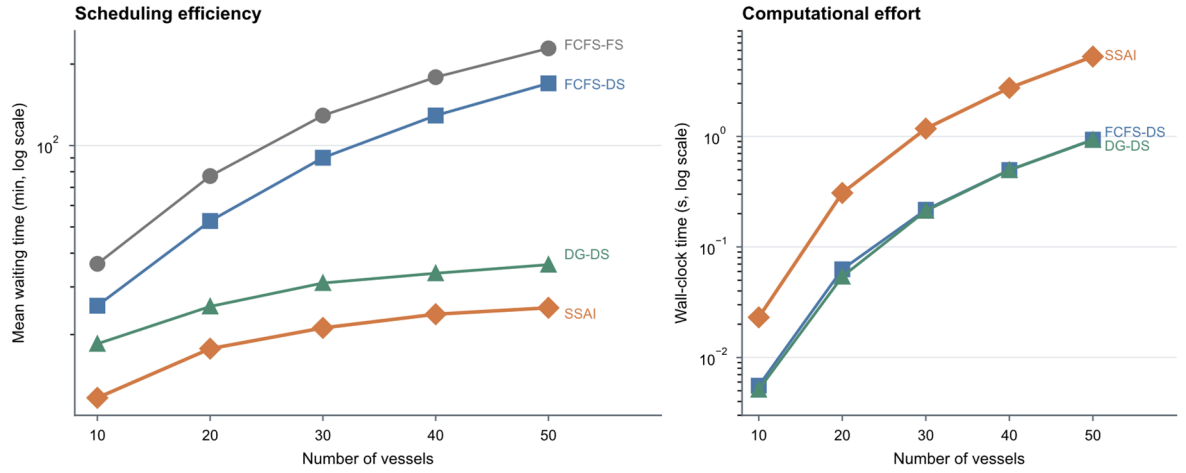

Figure 3. Scheduling efficiency and computational effort of the scheduling methods.

Table 4 shows successive waiting reductions as the scheduling decisions became more flexible. FCFS-DS reduced mean waiting by 25.7% to 31.8% relative to FCFS-FS, and direction grouping produced a further reduction. SSAI achieved the lowest observed mean waiting across the ten instances at each vessel count. Its reduction relative to DG-DS ranged from 29.4% to 36.9%, with the waiting curves separating further from the fixed order methods as vessel count grew. Moreover, SSAI obtained lower waiting than FCFS-DS in all 50 instances and lower waiting than DG-DS in 45 instances. Two-sided exact paired sign tests excluded ties and supported the SSAI-DG-DS difference at the 5% level for 20 to 50 vessels ($p \leq 0.0215$). For 10 vessels, excluding two ties left eight pairs: seven favoured SSAI and one favoured DG-DS ($p = 0.0703$). The lower mean at this size is therefore reported as an observed improvement trend. Meanwhile, Figure 3 shows the additional computation required by SSAI. Its mean runtime increased from 0.02 to 5.28 s across sizes, whereas FCFS-DS and DG-DS remained below 1 s at 50 vessels.

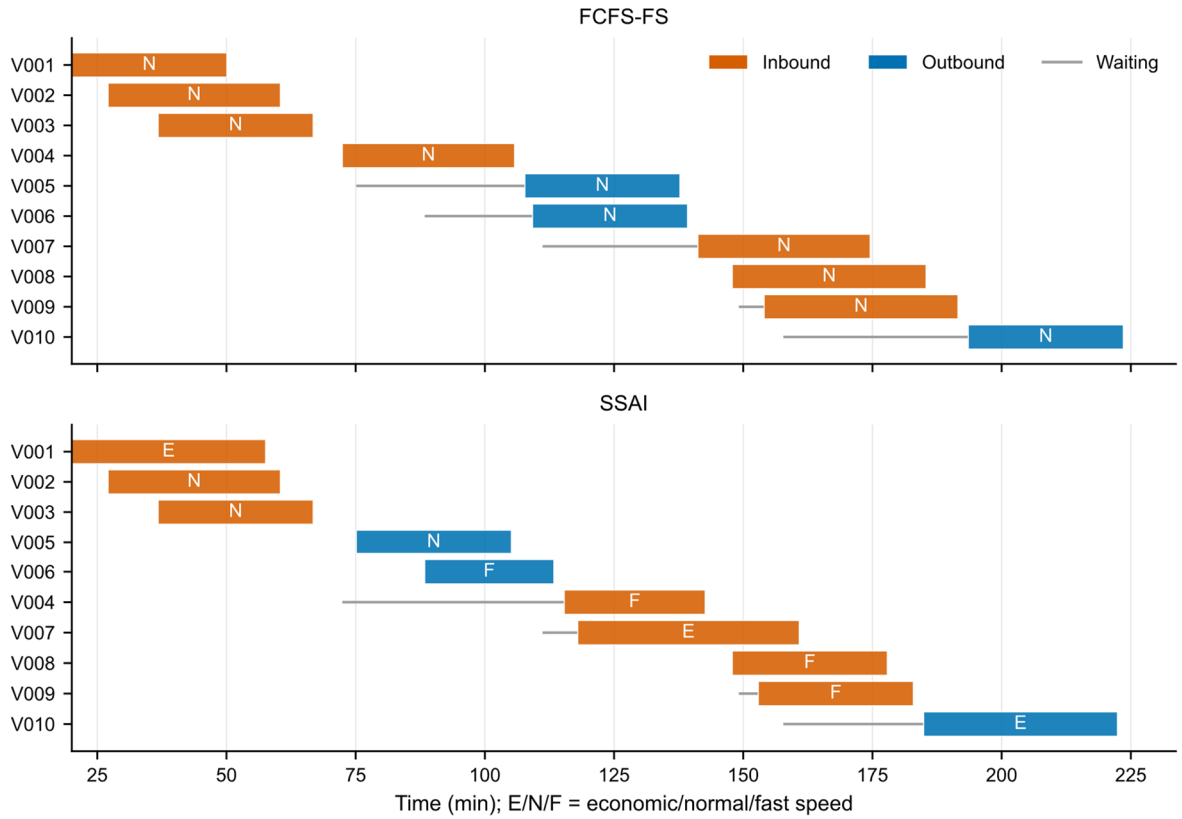

Figure 4. Gantt charts for a representative FCFS-FS and SSAI schedule.

These differences arise from how each method coordinates channel occupancy with subsequent release opportunities. Speed changes alter passage times and following headways even when the vessel order remains fixed. Direction grouping then reduces repeated clearance between opposing movements, while SSAI additionally revises vessel positions and group boundaries. Figure 4 illustrates these adjustments through different block starting times and following intervals in the representative schedule. In addition, Figure 5 shows that economic speed became less common as vessel count increased, while normal speed accounted for a larger share. The fast speed share also varied, consistent with selecting speeds in relation to neighbouring movements. Under the model, faster passage shortens occupancy but can increase the entry headway required for a following vessel. Consequently, the value of a speed change depends on its position in the release sequence. Evaluating more candidate placements explains the additional computation, while the combined decisions explain the observed waiting reductions.

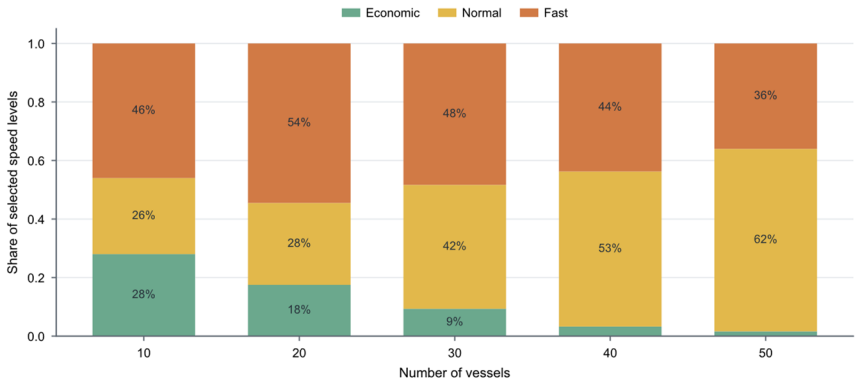

Figure 5. Distribution of speed choices under SSAI.

3.3. Small-Scale Exact Validation

To quantify the objective quality of SSAI, we conducted an exact validation experiment using MILP reference solutions. The experiment used 8, 10, 12 and 15 vessels, with ten seeds at each size giving 40 matched

comparisons. Both methods used identical objective coefficients and the same safety requirements. Every MILP run terminated with a proven optimum and zero reported MIP gap. Table 5 summarises the resulting gaps and runtimes, with the relative objective gap for instance r defined as follows:

$$g_r = 100 \times \frac{Z_r^{\mathrm{SSAI}} - Z_r^*}{Z_r^*}, \tag{40}$$

where Z_r^{SSAI} and Z_r^* denote the SSAI objective and proven MILP optimum for instance r, respectively. The gap is expressed as a percentage, and values within 10^{-6} of the optimum were counted as optimal hits. As Table 5 shows, SSAI matched the optimum in 16 of 40 instances, with a mean objective gap of 3.92%. However, the mean gap increased from 1.46% at eight vessels to 6.58% at 15 vessels, and the largest individual gap was 15.57%. Optimal hits also declined from five of ten instances at eight vessels to two of ten at 15 vessels. At the same time, SSAI required less mean computation time than exact solution at every tested size.

Table 5. Small-scale validation against proven MILP optima.

Number of Vessels	Instances	Mean Optimality Gap (%)	Maximum Gap (%)	Optimal Hits	Mean MILP Runtime (s)	Mean SSAI Runtime (s)
8	10	1.46	9.33	5/10	0.04	0.01
10	10	3.80	10.57	5/10	0.09	0.02
12	10	3.84	15.57	4/10	0.21	0.05
15	10	6.58	12.65	2/10	1.06	0.12

The increase in objective gaps is consistent with the growth in interacting order and speed choices as more vessels enter the scheduling problem. SSAI evaluates bounded neighbourhoods, so each iteration focuses on changes that directly improve the current schedule. This search structure keeps computation short while allowing useful adjustments to vessel positions and speed levels. As the number of interacting decisions grows, a larger share of the full solution space lies beyond those immediate adjustments. This relationship helps explain the declining frequency of optimal hits and the increasing mean gap. Overall, the exact comparison establishes how SSAI balances average objective quality with computational effort across the tested sizes.

3.4. Sensitivity to Safety Distance and Objective Weight

To examine performance under changing safety requirements and operating preferences, we conducted sensitivity experiments on ten matched instances containing 20 vessels. First, we scaled the base safety distance using $\eta_D \in \{0.75, 0.90, 1.00, 1.10, 1.25\}$, where 1.00 denotes the standard setting. Next, we varied α over 0, 0.05, 0.15, 0.50 and 1.50 to examine the preference between waiting and speed penalties. Each check changed one factor at a time, retaining seeds 1 to 10 and all other settings across the four methods. Tables 6 and 7 report the respective comparisons, while Figure 6 shows waiting and speed responses to safety distance. Figure 7 illustrates the standard safety headways across vessel types and speed combinations.

Table 6. Sensitivity to the safety distance factor.

Distance Factor	FCFS-FS Mean Waiting (min)	FCFS-DS Mean Waiting (min)	DG-DS Mean Waiting (min)	SSAI Mean Waiting (min)	SSAI Reduction vs. DG-DS
0.75	74.06	50.34	23.83	15.94	33.1%
0.90	75.90	51.64	24.76	17.21	30.5%
1.00	77.12	52.59	25.41	17.73	30.2%
1.10	78.35	53.56	26.04	17.76	31.8%
1.25	80.25	55.11	27.03	19.34	28.5%

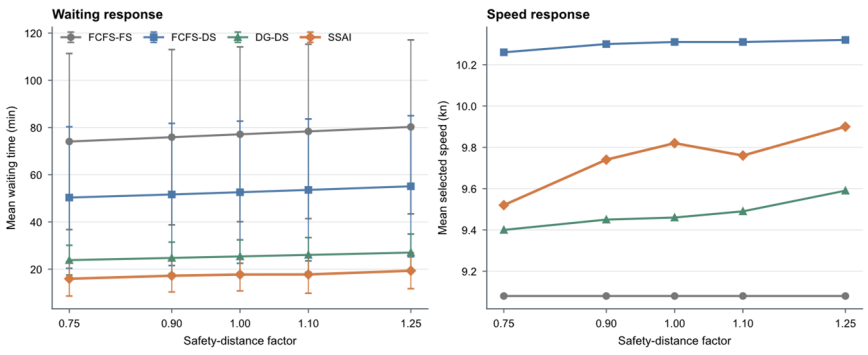

Figure 6. Sensitivity of the scheduling methods to the safety distance factor.

Table 6 shows that mean waiting increased with the prescribed safety distance for every method. SSAI's mean waiting rose by 21.4% between factors 0.75 and 1.25, yet remained 28.5% to 33.1% below DG-DS. Moreover, Figure 6 shows that DG-DS and SSAI achieved lower waiting at lower mean speeds than FCFS-DS. SSAI's mean speed varied from 9.52 to 9.90 kn, and mean runtime remained between 0.28 and 0.30 s. Error bars in the waiting panel denote one standard deviation over the ten matched instances. For the objective weight check, Table 7 shows that the comparative ranking remained stable. SSAI retained the lowest observed mean waiting at every tested weight, with values between 17.73 and 17.95 min. Increasing α from 0.15 to 1.50 reduced its mean penalty from 0.655 to 0.569 (13.1%), while mean waiting increased by 1.2%. Thus, the larger weight changed the selected operating balance while preserving SSAI's waiting advantage over the other methods.

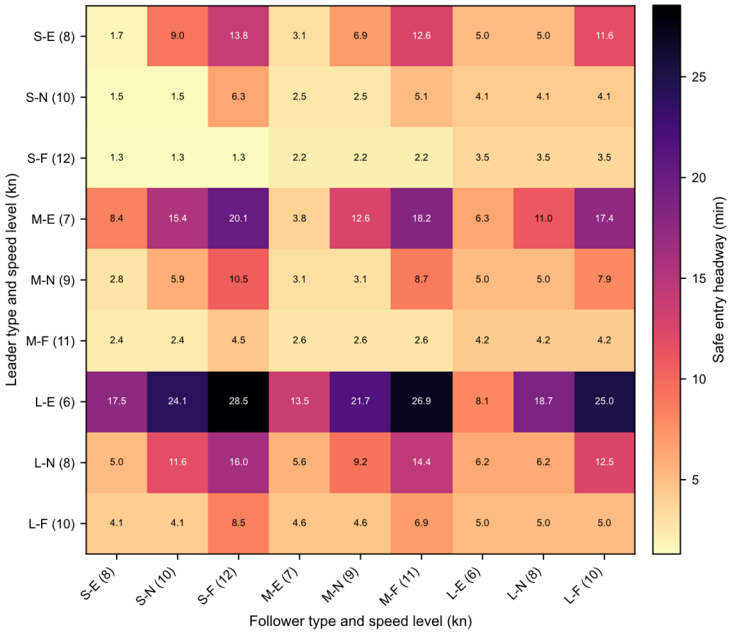

Figure 7. Safety headways (min), including the 0.5 min buffer ε_{ij}. Rows identify leaders and columns identify followers. S/M/L denote small/medium/large vessels; E/N/F denote economic/normal/fast speed levels. Parentheses give speeds in knots (kn).

Table 7. Mean waiting time (min) and SSAI speed penalty under different objective weights.

α	FCFS-FS	FCFS-DS	DG-DS	SSAI	SSAI Penalty
0.00	77.12	52.59	25.44	17.76	0.722
0.05	77.12	52.59	25.40	17.76	0.652
0.15	77.12	52.59	25.41	17.73	0.655
0.50	77.12	52.59	25.41	17.73	0.649
1.50	77.12	52.64	25.47	17.95	0.569

The two sensitivity responses have different explanations within the scheduling model. A larger safety distance increases the required separation, lengthening entry headways and reducing the opportunities to release following vessels. These delays can then propagate through the sequence, explaining the increase in waiting. As Figure 7 illustrates, the headway also depends on which vessel leads and how quickly its follower closes the distance. A faster follower behind a slower leader therefore requires a different entry interval from the reversed pairing. In comparison, changing α leaves the feasible headways fixed but changes how candidate schedules are valued. A larger weight favours lower speed penalties when candidate schedules have similar waiting times, explaining the observed shift in operating balance. The experiments therefore distinguish the effect of physical separation requirements from the effect of the scheduling preference. SSAI retained the lowest observed mean waiting as these factors changed.

3.5. Case Study with Engineering Parameters

To examine the scheduling approach at a practical channel scale, we conducted a case study using engineering parameters from Zhanjiang Port. The case adopted the public 16.9 km geometry of the project for vessels of 300,000 deadweight tonnes. We generated 30 vessels at four arrivals per hour. Small, medium and large vessels

had probabilities of 0.15, 0.35 and 0.50, respectively. Directions remained equiprobable, and the available speed levels followed Table 2. Table 8 compares all four methods using this channel geometry and generated traffic.

Table 8. Results for the Zhanjiang Port case with engineering parameters.

Method	Mean Waiting (min)	Maximum Waiting (min)	Throughput (vessels/h)	Direction Changes	Mean Speed (kn)	Runtime (s)
FCFS-FS	513.64	874.01	1.48	16	8.60	<0.01
FCFS-DS	398.94	692.52	1.74	16	9.93	0.21
DG-DS	65.58	144.50	3.90	4	9.53	0.18
SSAI	50.92	140.47	4.17	3	9.80	1.17

Table 8 shows that FCFS-DS reduced mean waiting by 22.3% relative to FCFS-FS, while both retained 16 direction changes. By contrast, DG-DS and SSAI reduced this count to four and three, respectively, alongside substantially lower mean waiting. SSAI reduced mean waiting by 90.1% relative to FCFS-FS and by 87.2% relative to FCFS-DS. Compared with DG-DS, SSAI further reduced mean waiting by 22.4% and maximum waiting by 2.8%. At the same time, throughput increased by 6.9%, from 3.90 to 4.17 vessels/h. Runtime increased from 0.18 to 1.17 s, linking these operational improvements to additional search effort. The greater reduction in mean than maximum waiting also distinguishes gains in average service from relief for the most delayed vessel.

The separation between fixed order and grouped schedules reflects the clearance required before each direction reversal. In this longer channel, each reversal requires opposing traffic to wait until the channel has cleared. Grouping compatible movements reduces these repeated clearance requirements, explaining the large waiting reduction relative to the fixed order methods. Within the resulting groups, SSAI further adjusts vessel positions and speeds to improve release timing under the required headways. Its additional candidate evaluations account for the higher runtime compared with simple direction grouping. Across the reported baseline comparisons, SSAI attained the lowest observed mean waiting through coordinated changes to release order and speed. Exact validation quantified the associated objective gaps, while sensitivity experiments separated the roles of safety requirements and operating preferences. Overall, these findings connect the algorithm's search decisions to improved channel use.

4. Discussion

Sailing speed determines both transit duration and the safety interval between successive vessel entries. A faster vessel completes its passage sooner, while a faster follower closes the distance to its leader during transit. The entry headway must account for this relative motion to maintain safe separation. The proposed model links each headway to the selected speeds of both vessels and incorporates that relationship into scheduling. With each vessel maintaining its selected speed, the headway preserves the required separation throughout their shared channel occupancy. This formulation connects an individual speed choice to its consequences for subsequent vessel releases. Channel efficiency therefore depends on how vessel speeds interact across the release sequence.

Jointly adjusting vessel order and speed improves the use of these release opportunities. Direction grouping reduces the repeated clearance required before opposing traffic can enter. Within each group, vessel order and relative speeds determine the timing of successive entries. SSAI adjusts both decisions and achieved lower observed mean waiting than the direction grouping baseline. The additional improvement shows the value of coordinating movements within release groups as well as arranging the groups themselves. Group composition determines direction changes, while vessel order and speed determine successive entry intervals. Coordinating these decisions improves the timing of the complete release schedule. Exact validation also showed that SSAI produced solutions close to the optimum on average and reduced computation time relative to exact solution.

The sensitivity experiments further show that efficient scheduling can combine lower waiting with lower average sailing speeds. Direction grouping and SSAI achieved this combination relative to speed adjustment under a fixed order, highlighting the importance of release timing. Increasing the weight on the normalised speed penalty also reduced that penalty with little change in mean waiting. In contrast, increasing the prescribed safety distance raised waiting across all methods. These responses distinguish two management decisions. Safety requirements determine the permissible entry intervals, while operating preferences guide the choice among feasible schedules. Port managers can use this distinction to compare release plans and select speed instructions that balance waiting and speed penalties. The resulting decisions coordinate individual vessel movements with the timing of the complete release sequence.

5. Conclusions and Managerial Implications

This study developed a joint scheduling approach for single-lane bidirectional port channels in which vessel speed determines both transit time and safe entry separation. A continuous-time MILP coordinates vessel order with entry times and discrete speed choices to minimise waiting while accounting for a normalised speed penalty. For following vessels, the headway derives from relative motion throughout transit; for opposing vessels, the model requires channel clearance before the direction changes. Precomputed headways and exact linearisation incorporate these interactions into a common mathematical formulation. Building on this formulation, SSAI alternates between resequencing vessels and adjusting speeds, evaluating each candidate timetable under the same objective and safety rules. The resulting contribution is a consistent connection between the physical requirements for safe passage and the decisions used to improve the schedule. Across the baseline comparisons, SSAI achieved the lowest observed mean waiting at each tested vessel count. Exact validation quantified its average objective gap and computational savings relative to proven MILP solutions. The sensitivity experiments further showed that its waiting advantage persisted across the tested safety distances and objective weights.

For port managers, the findings support coordinating release order and speed instructions when allocating access to a shared channel. In particular, direction grouping addresses repeated clearance, while adjustments within the sequence improve the timing of successive movements under the required headways. Managers can therefore use the resulting schedules to compare release plans and assess how operating preferences affect waiting and speed penalties. The prescribed safety parameters remain part of every candidate evaluation, linking these comparisons to local navigation requirements. A natural next step is to incorporate updated AIS arrival information into repeated planning and evaluate the resulting release decisions under operational uncertainty. This extension would connect the present scheduling approach to the continuing adjustment of vessel access plans in port traffic management.

Author Contributions

C.G.: Conceptualization, Methodology, Software, Formal analysis, Investigation, Data curation, Visualization, Writing—original draft, Writing—review & editing. Y.L.: Validation, Formal analysis, Investigation, Data curation, Visualization, Writing—review & editing. Y.Z.: Conceptualization, Methodology, Validation, Supervision, Project administration, Funding acquisition, Writing—review & editing. All authors have read and agreed to the published version of the manuscript.

Funding

This work was supported by The Hong Kong Polytechnic University under Grant P0053253.

Institutional Review Board Statement

Not applicable.

Informed Consent Statement

Not applicable.

Data Availability Statement

Data will be made available upon reasonable request.

Conflicts of Interest

The authors declare no conflict of interest. They have no known competing financial interests or personal relationships that could have appeared to influence the work reported in this paper.

Use of AI and AI-Assisted Technologies

Generative artificial intelligence tools were used solely to support language editing and document formatting. The authors reviewed all revisions and take full responsibility for the content of the manuscript.

References

1. United Nations Conference on Trade and Development (UNCTAD). Review of Maritime Transport 2024: Navigating Maritime Chokepoints; United Nations: Geneva, Switzerland, 2024. Available online: https://unctad.org/publication/review-maritime-transport-2024 (accessed on 28 October 2026).
2. Lübbecke, E.; Lübbecke, M.E.; Möhring, R.H. Ship Traffic Optimization for the Kiel Canal. *Oper. Res.* **2019**, *67*, 791–812. https://doi.org/10.1287/opre.2018.1814.
3. National Development and Reform Commission. Approval of the Feasibility Study Report for the 300,000-Tonne Channel Reconstruction and Expansion Project of Zhanjiang Port (NDRC Infrastructure [2018] No. 1017). 2018. Available online: https://www.ndrc.gov.cn/xxgk/zcfb/pifu/201810/t20181009_1316132.html (accessed on 28 October 2026).
4. Meisel, F.; Fagerholt, K. Scheduling two-way ship traffic for the Kiel Canal: Model, extensions and a matheuristic. *Comput. Oper. Res.* **2019**, *106*, 119–132. https://doi.org/10.1016/j.cor.2019.02.015.
5. City of Kiel. Kieler Zahlen 2025: Chapter 7, Hafen und Verkehr, Table 707 [Kiel Statistics 2025: Harbour and Transport, ship traffic on the Kiel Canal]. Available online: https://kiel.de/de/kiel_zukunft/statistik_kieler_zahlen/_dokumente/7._Hafen_und_Verkehr.pdf (accessed on 28 October 2026). (In German)
6. Office of Port of Entry and Exit of Shenzhen Municipal People's Government. Shenzhen Channel Scheduling Optimisation Agent: A Case of Improving Port Services. 2026. Available online: https://ka.sz.gov.cn/ztzl/szkaghjs/news/content/post_12671184.html (accessed on 28 October 2026).
7. Lalla-Ruiz, E.; Shi, X.; Voß, S. The waterway ship scheduling problem. *Transp. Res. Part D Transp. Environ.* **2018**, *60*, 191–209. https://doi.org/10.1016/j.trd.2016.09.013.
8. Hill, A.; Lalla-Ruiz, E.; Voß, S.; et al. A multi-mode resource-constrained project scheduling reformulation for the waterway ship scheduling problem. *J. Sched.* **2019**, *22*, 173–182. https://doi.org/10.1007/s10951-018-0578-9.
9. Liu, B.; Li, Z.C.; Sheng, D.; et al. Integrated planning of berth allocation and vessel sequencing in a seaport with one-way navigation channel. *Transp. Res. Part B Methodol.* **2021**, *143*, 23–47. https://doi.org/10.1016/j.trb.2020.10.010.
10. Zhang, X.; Lin, J.; Guo, Z.; et al. Vessel transportation scheduling optimization based on channel–berth coordination. *Ocean. Eng.* **2016**, *112*, 145–152. https://doi.org/10.1016/j.oceaneng.2015.12.011.
11. Xu, Y.; Xue, K.; Du, Y. Berth Scheduling Problem Considering Traffic Limitations in the Navigation Channel. *Sustainability* **2018**, *10*, 4795. https://doi.org/10.3390/su10124795.
12. Corry, P.; Bierwirth, C. The Berth Allocation Problem with Channel Restrictions. *Transp. Sci.* **2019**, *53*, 708–727. https://doi.org/10.1287/trsc.2018.0865.
13. Jia, S.; Li, C.L.; Xu, Z. Managing Navigation Channel Traffic and Anchorage Area Utilization of a Container Port. *Transp. Sci.* **2019**, *53*, 728–745. https://doi.org/10.1287/trsc.2018.0879.
14. Abou Kasm, O.; Diabat, A.; Bierlaire, M. Vessel scheduling with pilotage and tugging considerations. *Transp. Res. Part E Logist. Transp. Rev.* **2021**, *148*, 102231. https://doi.org/10.1016/j.tre.2021.102231.
15. Petris, M.; Pellegrini, P.; Pesenti, R. Models and algorithms for an integrated vessel scheduling and tug assignment problem within a canal harbor. *Eur. J. Oper. Res.* **2022**, *300*, 1120–1135. https://doi.org/10.1016/j.ejor.2021.10.037.
16. Jiang, X.; Zhong, M.; Shi, J.; et al. Overall Scheduling Model for Vessels Scheduling and Berth Allocation for Ports with Restricted Channels That Considers Carbon Emissions. *J. Mar. Sci. Eng.* **2022**, *10*, 1757. https://doi.org/10.3390/jmse10111757.
17. Muñuzuri, J.; Barbadilla, E.; Escudero-Santana, A.; et al. Planning Navigation in Inland Waterways with Tidal Depth Restrictions. *J. Navig.* **2018**, *71*, 547–564. https://doi.org/10.1017/s0373463317000789.
18. Zhang, B.; Zheng, Z. Model and Algorithm for Vessel Scheduling through a One-Way Tidal Channel. *J. Waterw. Port Coast. Ocean. Eng.* **2020**, *146*, 04019032. https://doi.org/10.1061/(asce)ww.1943-5460.0000545.
19. Zhang, B.; Zheng, Z.; Wang, D. A model and algorithm for vessel scheduling through a two-way tidal channel. *Marit. Policy Manag.* **2020**, *47*, 188–202. https://doi.org/10.1080/03088839.2019.1676477.
20. Nehrke, L.; Schulz, A. Scheduling of waterways with tide and passing box. *Nav. Res. Logist. NRL* **2022**, *69*, 609–621. https://doi.org/10.1002/nav.22033.
21. Zhao, K.; Jin, J.G.; Zhang, D.; et al. A variable neighborhood search heuristic for real-time barge scheduling in a river-to-sea channel with tidal restrictions. *Transp. Res. Part E Logist. Transp. Rev.* **2023**, *179*, 103280. https://doi.org/10.1016/j.tre.2023.103280.
22. Gan, S.; Wang, Y.; Li, K.; et al. Efficient online one-way traffic scheduling for restricted waterways. *Ocean. Eng.* **2021**, *237*, 109515. https://doi.org/10.1016/j.oceaneng.2021.109515.
23. Liu, D.; Shi, G.; Kang, Z. Fuzzy Scheduling Problem of Vessels in One-Way Waterway. *J. Mar. Sci. Eng.* **2021**, *9*, 1064. https://doi.org/10.3390/jmse9101064.
24. Zhen, R.; Sun, M.; Fang, Q. Optimization of Inbound and Outbound Vessel Scheduling in One-Way Channel Based on Reinforcement Learning. *J. Mar. Sci. Eng.* **2025**, *13*, 237. https://doi.org/10.3390/jmse13020237.

25. Fagerholt, K.; Laporte, G.; Norstad, I. Reducing fuel emissions by optimizing speed on shipping routes. *J. Oper. Res. Soc.* **2010**, *61*, 523–529. https://doi.org/10.1057/jors.2009.77.
26. Xia, Z.; Guo, Z.; Wang, W.; et al. Joint optimization of ship scheduling and speed reduction: A new strategy considering high transport efficiency and low carbon of ships in port. *Ocean. Eng.* **2021**, *233*, 109224. https://doi.org/10.1016/j.oceaneng.2021.109224.
27. Liu, B.; Wang, X.; Wang, Z.; et al. Modeling and solving the joint berth allocation and vessel sequencing problem with speed optimization in a busy seaport. *Transp. Res. Part E Logist. Transp. Rev.* **2025**, *197*, 104089. https://doi.org/10.1016/j.tre.2025.104089.
28. Du, J.; Lin, S.; Guo, L.; et al. Machine learning-based adaptive large neighborhood search algorithm for the integrated vessel scheduling and speed optimization problem in the compound channel. *Appl. Soft Comput.* **2025**, *185*, 113980. https://doi.org/10.1016/j.asoc.2025.113980.
29. Liu, D.; Shi, G.; Hirayama, K. Vessel Scheduling Optimization Model Based on Variable Speed in a Seaport with One-Way Navigation Channel. *Sensors* **2021**, *21*, 5478. https://doi.org/10.3390/s21165478.